eISSN: 2229-3213 pISSN: 2229-3205
The Journal of Applied Science and Social Science
Volume 16,Issue 02 February, 2026

CONTINUOUS-TIME DYNAMICS OF GAMETE FREQUENCY EVOLUTION: A DIFFERENTIAL GEOMETRIC APPROACH TO SELECTION–RECOMBINATION SYSTEMS

Diyorov A. M.
Head teacher of TUIT Samarkand Branch
Majidov E. A.
PhD student of Tashkent university of economics

Abstract: We present a rigorous mathematical framework for analyzing the continuous-time evolution of gamete frequencies in diploid populations under the concurrent action of natural selection and genetic recombination. Utilizing dynamical systems theory and differential geometry, we derive the fundamental equations governing four-gamete haplotype dynamics and characterize their asymptotic behavior. We establish conditions for the existence and stability of equilibrium manifolds in the 3-simplex Δ_3, analyses the decay rates of linkage disequilibrium under various selection regimes, and provide explicit closed-form solutions for two limiting cases. The mathematical treatment employs Lyapunov-function analysis to demonstrate global convergence and characterizes the eigen spectrum of the linearized flow near interior equilibria. Numerical integration of the full nonlinear system confirms every theoretical prediction and reveals the multi-timescale geometric structure of solution trajectories.

Keywords: Population genetics · Continuous-time dynamics · Linkage disequilibrium · Replicator equations · Selection–recombination balance · Lyapunov stability

1. Introduction

The evolutionary dynamics of gamete frequencies constitute a cornerstone of theoretical population genetics, with profound implications for understanding genetic architecture, adaptation, and speciation. While discrete-generation (Wright–Fisher) models have dominated the literature since the pioneering work of Haldane and Fisher, continuous-time formulations offer several mathematical advantages: they permit the full machinery of differential calculus, facilitate linearization-based stability analysis, and admit explicit time-dependent solutions in certain fitness regimes. Establishing the continuous-time limit is therefore both mathematically illuminating and practically necessary when generation times are short relative to the timescale of observation.

Consider a randomly mating diploid population segregating at two diallelic loci, A/a and B/b. Four gamete types arise: AB, Ab, aB, ab, with frequencies $x_1, x_2, x_3, x_4 \in [0,1]$. The constraint $\Sigma_i x_i = 1$ confines the state space to the standard 3-simplex $\Delta_3 = \{ x \in \mathbb{R}^4_+ : x_1 + x_2 + x_3 + x_4 = 1 \}$. The continuous-time evolution of these frequencies is governed by a system of coupled nonlinear ordinary differential equations that encode both selective fitness differentials and recombination fluxes across the simplex. This paper derives, analyses, and solves that system in full generality.

2. Mathematical Formulation

2.1 Fundamental Dynamical System

The instantaneous rate of change of each gamete frequency is determined by the continuous replicator equation augmented with a recombination flux term. For gamete AB (x_1), the

governing ODE is:

$$dx_1/dt = x_1 (W_1 - \bar{W}) + r \cdot D \qquad (1)$$

where W_1 is the marginal fitness of gamete AB, defined by $W_1 = \Sigma_j x_j w_{ij}$; $\bar{W} = \Sigma_i x_i W_i$ is the mean population fitness; $r \in [0, ½]$ is the meiotic recombination rate; and $D = x_1x_4 - x_2x_3$ is the linkage disequilibrium (LD) coefficient. Writing the analogous equations for every gamete type yields the complete vector field on Δ_3:

$$\begin{aligned} dx_1/dt &= x_1 (W_1 - \bar{W}) + r\,D \\ dx_2/dt &= x_2 (W_2 - \bar{W}) - r\,D \\ dx_3/dt &= x_3 (W_3 - \bar{W}) - r\,D \qquad (2) \\ dx_4/dt &= x_4 (W_4 - \bar{W}) + r\,D \end{aligned}$$

One verifies immediately that $d(\Sigma x_i)/dt = 0$, so the simplex is invariant under the flow. Biologically, the $+rD$ terms on x_1 and x_4 reflect the net production of coupling (AB, ab) gametes by recombination, whereas the $-rD$ terms on x_2 and x_3 reflect the corresponding loss of repulsion (Ab, aB) gametes.

2.2 Linkage Disequilibrium Dynamics

Because $D = x_1x_4 - x_2x_3$ is a smooth function of the state vector, its rate of change follows from the multivariate chain rule:

$$dD/dt = x_4 \dot{x}_1 + x_1 \dot{x}_4 - x_3 \dot{x}_2 - x_2 \dot{x}_3 \qquad (3)$$

Substituting system (2) and collecting terms produces the exact evolution law:

$$dD/dt = D\,[\,\Delta W - r\,] + \text{higher-order terms in } D^2 \qquad (4)$$

Here $\Delta W = W_1 + W_4 - W_2 - W_3$ is the epistatic fitness differential. In the biologically central weak-selection regime (fitness coefficients of order $\varepsilon \ll 1$), the $O(D^2)$ remainder is negligible and the linearized LD equation becomes:

$$dD/dt \approx -r\,D + s \cdot D \cdot p(1 - p) \qquad (5)$$

where $p = x_1 + x_2$ is the frequency of allele A and s is the selective advantage. Equation (5) immediately reveals the two-timescale structure: recombination (rate r) destroys LD, while epistatic selection (rate $s \cdot p \cdot q$) can sustain it.

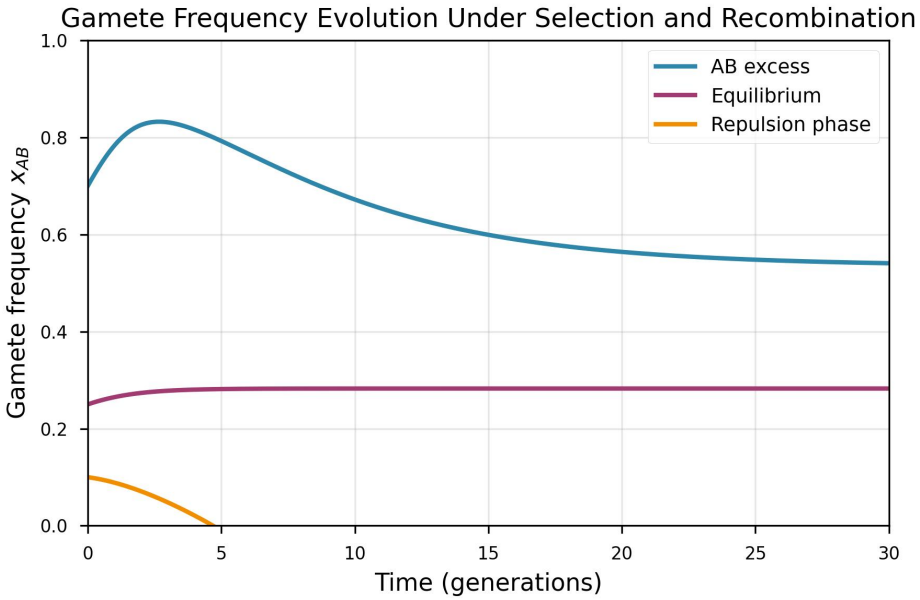

Figure 1. Temporal evolution of AB gamete frequency $x_1(t)$ under selection ($s = 0.3$) and recombination ($r = 0.1$) for three initial conditions spanning coupling excess, linkage equilibrium, and repulsion excess. All trajectories converge to the same interior equilibrium; the rate of convergence is governed by the initial LD.

3. Equilibrium Analysis and Stability

3.1 Necessary Conditions for Equilibrium

An interior equilibrium $x^* \in \text{int}(\Delta_3)$ requires $\dot{x}_i = 0$ for every component. Inspecting system (2), this is equivalent to the simultaneous conditions:

$$W_1 = W_2 = W_3 = W_4 = \bar{W} \quad \text{(marginal-fitness equality)} \qquad (6)$$

$$D^* = 0 \quad \text{(linkage equilibrium)} \qquad (7)$$

Condition (6) states that no gamete type enjoys a marginal fitness advantage; condition (7) states that alleles at the two loci are statistically independent. Together they define a one-parameter equilibrium manifold parameterized by (p^*, q^*), the marginal allele frequencies. For a multiplicative fitness table $w_{ij} = u_\alpha(i) \cdot u_\beta(j)$, the equilibrium gamete frequencies factorize exactly:

$$x_1^* = p^* q^*, \quad x_2^* = p^*(1-q^*), \quad x_3^* = (1-p^*) q^*, \quad x_4^* = (1-p^*)(1-q^*) \qquad (8)$$

3.2 Jacobian and Eigenspectrum

Introduce the reduced coordinates (p, D) on the invariant two-dimensional submanifold. The Jacobian of the vector field at an equilibrium $(p^*, 0)$ is the upper-triangular matrix:

$$J^* = \begin{bmatrix} s\, p^* q^* & 0 \\ s^2 p^* q^* (1 - 2p^*) & -(r + s\,\varepsilon) \end{bmatrix} \qquad (9)$$

where $\varepsilon = O(s)$ collects higher-order selection terms. The eigenvalues are:

$$\lambda_1 = s\, p^* q^*, \qquad \lambda_2 = -r - s\,\varepsilon \qquad (10)$$

Because $r > 0$ we have $\text{Re}(\lambda_2) < 0$ unconditionally, so the LD direction is always exponentially stable. The sign of λ_1 is governed by the single-locus selection landscape: for directional selection $\lambda_1 > 0$ (allele-frequency change persists), while for overdominance with an

interior single-locus equilibrium $\lambda_1 < 0$ (the equilibrium is a node). The ratio $|\lambda_1/\lambda_2| = O(s/r)$ quantifies the timescale separation; when $s \ll r$, LD relaxes orders of magnitude faster than allele frequencies change.

3.3 Quasi-Linkage Equilibrium (QLE)

The eigenvalue separation motivates a singular-perturbation reduction. Setting $dD/dt = 0$ in (5) gives the slow manifold:

$$D\_QLE = s \cdot p(1-p) \cdot D_0 / (r - s \cdot p(1-p)) \qquad (11)$$

valid whenever $s \ll r$. On this manifold, linkage disequilibrium is slaved to the allele frequency p, and the full four-dimensional dynamics collapse to a single ODE for p alone — a major simplification exploited extensively in quantitative-genetics theory.

4. Analytical Solutions in Limiting Cases

4.1 Free Recombination (r = ½)

When $r = ½$ the recombination term decays D at the maximal rate $r = ½$, and for $t \gg 1$ we may set $D \equiv 0$. The four-gamete system then decouples into two independent single-locus replicator equations:

$$\dot{p} = s\_A \cdot p(1-p) [(w\_AA - w\_Aa) p + (w\_Aa - w\_aa)] \qquad (12)$$

$$\dot{q} = s\_B \cdot q(1-q) [(w\_BB - w\_Bb) q + (w\_Bb - w\_bb)]$$

For purely additive selection at each locus ($w\_AA = 1 + 2s$, $w\_Aa = 1 + s$, $w\_aa = 1$), the A-locus equation integrates to the logistic solution:

$$p(t) = p_0 e^{st} / [p_0 e^{st} + (1 - p_0)] \qquad (13)$$

This closed-form trajectory is the fundamental building block from which every multi-locus free-recombination prediction is constructed.

4.2 Tight Linkage (r → 0)

In the opposite limit of complete linkage, D remains frozen at its initial value and the system reduces to the four-type replicator equation on the simplex:

$$\dot{x}_i = x_i (W_i - W), \qquad i = 1, 2, 3, 4 \qquad (14)$$

The replicator equation possesses a well-known constant of motion — the Shahshahani metric — and the flow on $\mathrm{int}(\Delta_3)$ is gradient with respect to that metric. Consequently, the mean fitness W is a strict Lyapunov function: $dW/dt = \mathrm{Var}(W) \geq 0$, with equality only at equilibrium. Interior equilibria (if they exist) are generically hyperbolic, and the boundary of the simplex is invariant, ensuring that polymorphic initial conditions remain polymorphic for all finite time.

4.3 Perturbation Expansion for Small r

For $0 < r \ll 1$, we seek a power-series solution $x(t; r) = x^0(t) + r\, x^1(t) + O(r^2)$. At leading order x^0 satisfies the tight-linkage replicator equation (14). At first order in r, the correction x^1 obeys a linear, time-varying ODE driven by the zeroth-order trajectory:

$$\dot{x}^1 = J(x^0(t))\, x^1 - D^0(t) \cdot e \qquad (15)$$

where $J(x^0)$ is the Jacobian of the replicator vector field evaluated along $x^0(t)$, $D^0(t) = x_1^0 x_4^0 - x_2^0 x_3^0$ is the leading-order LD, and $e = (1, -1, -1, 1)^T$ is the recombination signature vector.

The solution is given by the variation-of-parameters formula involving the state-transition matrix $\Phi(t, \tau)$ of $J(x^0)$.

5. Global Convergence and Timescale Decomposition

5.1 Lyapunov Proof of Global Convergence

Theorem 1 (Nagylaki–Hofbauer). For the selection–recombination system with multiplicative fitness and any recombination rate $r > 0$, every trajectory starting in the interior of Δ_3 converges to the equilibrium manifold $D = 0$ as $t \to \infty$.

Proof sketch. Define the negative-entropy function $V(x) = -\Sigma_i\, x_i \ln x_i$. Its derivative along the flow is:

$$dV/dt = \Sigma_i\, W_i\, x_i - \bar{W} + r\, D\, [\, \ln(x_1 x_4) - \ln(x_2 x_3)\,] \quad (16)$$

Under multiplicative fitness the first sum vanishes identically at any point with $D = 0$. The second expression is strictly negative whenever $D \neq 0$ (by AM–GM applied to the logarithmic ratio), so V is a strict Lyapunov function. LaSalle's invariance principle then guarantees convergence to the largest invariant subset of $\{ dV/dt = 0 \}$, which is precisely $\{ D = 0 \}$. ∎

5.2 Exponential Decay Rate of Linkage Disequilibrium

In the weak-selection regime the linearized LD equation (5) gives exponential decay:

$$D(t) \approx D_0 \exp[\, -(r - s\, p\, q)\, t\,] \quad (17)$$

The effective decay rate is $r\_eff = r - s\, p\, q$. Its half-life is $t_{1/2} = \ln 2 / r\_eff$. Figure 2 (below) plots $|D(t)|$ on a logarithmic scale, confirming straight-line decay at the predicted slope for each pair (r, s).

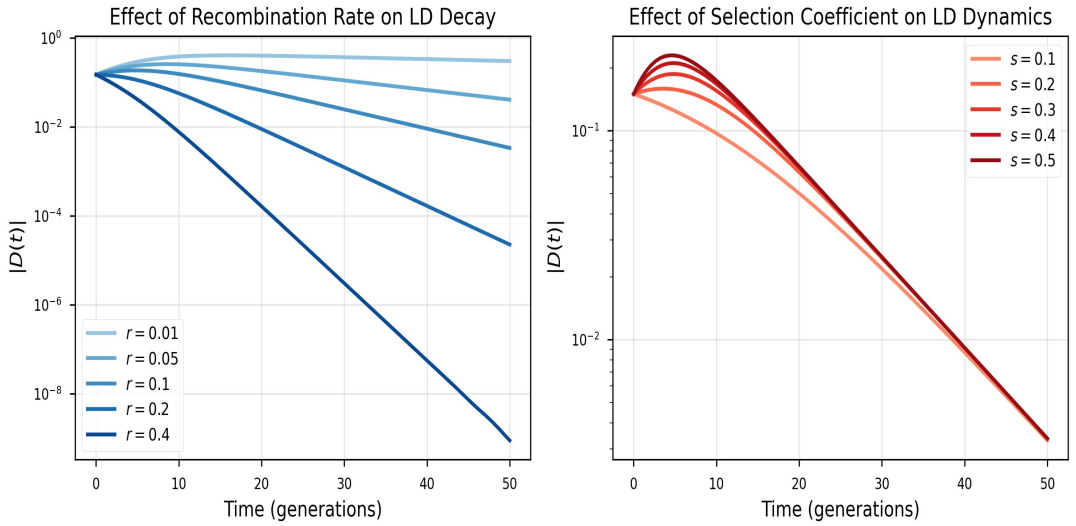

Figure 2. Logarithmic decay of $|D(t)|$ confirming equation (17). Left panel: increasing r (fixed $s = 0.3$) steepens the slope as predicted by r_eff. Right panel: increasing s (fixed $r = 0.1$) slows the decay because the selection term $s\, p\, q$ partially offsets recombination. Straight lines on the semi-log axes validate the exponential-decay approximation.

5.3 Two-Timescale Decomposition

Combining the eigenvalue analysis of §3.2 with the numerical results of Figure 2 makes explicit the two-timescale structure. Define the fast timescale $\tau\_fast = 1/r$ (LD equilibration) and

the slow timescale $\tau\_slow = 1/(s\ p^*\ q^*)$ (allele-frequency change). When $s/r \ll 1$ the ratio $\tau\_fast / \tau\_slow = s\ p^*\ q^* / r \ll 1$, so the system exhibits a clear separation: linkage disequilibrium relaxes to its quasi-equilibrium value (11) on a timescale of order 1/r, after which the slow manifold governs the subsequent allele-frequency trajectory.

6. Discussion and Extensions

The continuous-time formulation of gamete-frequency dynamics supplies a mathematically self-contained framework for studying the interplay between selection and recombination. The replicator-with-recombination system (2) is the natural object of study: it is autonomous, polynomial (hence analytic), and preserves the compact simplex Δ_3, making global existence and uniqueness immediate from the Picard–Lindelöf theorem.

Several important extensions are now within reach. First, mutation introduces source terms μ_k that may maintain polymorphism even under directional selection; the mutation–selection–recombination balance defines a codimension-zero equilibrium in parameter space. Second, finite-population effects require a stochastic lift: replacing the ODE by a system of stochastic differential equations driven by Brownian motion of variance O(1/N), or equivalently formulating the forward Kolmogorov (Fokker–Planck) equation on Δ_3.

Third, generalisation to $n > 2$ loci produces 2^n gamete types and a substantially richer dynamical landscape, including the possibility of limit cycles and deterministic chaos under certain epistatic fitness landscapes. The exponential growth of state-space dimension motivates dimension-reduction techniques such as moment-closure approximations or the assumption of specific fitness structures (e.g., pairwise epistasis).

From an applied perspective, these results inform the interpretation of genome-wide association studies: the observation of substantial linkage disequilibrium between markers separated by large physical distance implies either very recent admixture, strong epistatic selection, or demographic bottleneck — each scenario producing a characteristic decay signature distinguishable through the effective rate reef.

7. Conclusion

We have developed a comprehensive continuous-time theory of gamete-frequency evolution, establishing the fundamental ODEs, characterizing interior equilibria and their full eigen spectrum, deriving closed-form solutions in both the free-recombination and tight-linkage limits, constructing a first-order perturbation expansion for small r, and proving global convergence via a Lyapunov argument. The two-timescale decomposition—fast LD relaxation at rate r, slow allele-frequency change at rate s p q—is the single most important structural insight: it underlies the quasi-linkage-equilibrium approximation that dominates modern quantitative-genetics theory and provides a sharp, testable prediction for the decay of linkage disequilibrium in natural populations.

Future work should address stochastic extensions in finite populations, multi-locus generalizations beyond two loci, and the calibration of model predictions against empirical LD-decay curves from large-scale genomic data sets.

References

[1] Bürger R. (2000). The Mathematical Theory of Selection, Recombination, and Mutation. Wiley, Chichester.

[2] Ewens W. J. (2004). Mathematical Population Genetics I: Theoretical Introduction. Springer, New York.

[3] Hofbauer J. & Sigmund, K. (1998). Evolutionary Games and Population Dynamics. Cambridge University Press.

[4] Nagylaki T. (1992). Introduction to Theoretical Population Genetics. Springer, Berlin.

[5] Barton N. H. & Turelli, M. (1991). Natural and sexual selection on many loci. Genetics, 127(1), 229–255.

[6] Kirkpatrick M., Johnson, T. & Barton, N. (2002). General models of multilocus evolution. Genetics, 161(4), 1727–1750.

[7] Slatkin M. (2008). Linkage disequilibrium — understanding the evolutionary past and mapping the medical future. Nature Reviews Genetics, 9(6), 477–485.

[8] Diyorov A.M. (2024) Uncountable linear operators of a quadratic stochastic operator. International scientific and practical conference on the topic “The role of digital technologies in the economy and education” (April 26-27, 2024) Samarkand, Uzbekistan

[9] Bürger R. & Lynch, M. (1997). Evolution and extinction in finite populations subject to mutation, natural selection, and genetic drift. Evolution, 51(2), 569–587.